

Study of seismic response of colluvium accumulation slope by particle flow code

Jianming He · Xiao Li · Shouding Li ·
Yueping Yin · Haitao Qian

Received: 15 December 2009 / Published online: 19 September 2010
© Springer-Verlag 2010

Abstract Colluvium accumulation slopes (CAS) are widely distributed in Sichuan Province of China, especially in the regions with intense earthquake histories. These kinds of accumulations show obvious discontinuous and heterogeneous characteristics, to which the discrete element method (DEM) for discontinuous material is more suitably applied. Wenchuan earthquake with a magnitude of 8.0, caused a large number of debris flows or landslides in the colluvium formations, which are densely distributed in the quake-hit region in Sichuan province. The dynamic response of CAS is a key problem for study of stability of these kinds of slope. In this paper, PFC (Particle Flow Code) from Itasca based on DEM is used for modeling the dynamic response of the colluvium accumulations and some typical models were built according to the geological investigations carried out in the epicentral area. Horizontal shearing waveforms of WenChuan earthquake were input into the model for the study of the dynamic response of overlying colluvium accumulation and bedrock. The modeling results of different models under the same seismic conditions are described and analyzed at the end of the paper.

Keywords Colluvium accumulation slope (CAS) · Dynamic response · Particle flow code · Discontinuous characteristics

1 Introduction

Colluvium accumulation slopes (CAS) are widely distributed in Sichuan Province of China, which has undergone several intense seismic shocks in its history, especially the recent well known WenChuan Earthquake with a magnitude of 8.0 on the Richter scale. The intense shaking happened in a densely populated mountainous region and caused a large number of landslides, which inflicted great damage to the roads and buildings. The quake also triggered a large number of debris flows or landslides occurring in the overlying colluvium accumulations, which are densely distributed in the quake-hit region. These kinds of debris flows or slope instabilities in quake-hit areas have resulted in tremendous loss of life and property worldwide. Figure 1 exhibits a typical debris flow occurring in the overlying accumulation along a main road.

These colluvium accumulations have been formed due to the movement of earth crust, cutting, weathering, degradation and transportation caused by river streams during the later Tertiary period, especially the Quaternary period. Earthquakes often play the role of expediting the formation process.

According to the geological investigation carried out in the epicentral area after the quake, the thickness of most of the overlying colluvium accumulation is generally within 20 m and height of the bedrock keep in the range of 50–100 m. Typical profile of this kind of slope is plotted in the Fig. 2.

There are a wide range of substances including soil, sand, rock fragments with varying degrees of weathering that

J. He · X. Li · S. Li (✉)
Key Laboratory of Engineering Geomechanics, Institute
of Geology and Geophysics, Chinese Academy of Sciences,
Beijing 100029, People's Republic of China
e-mail: lsdlyh@mail.iggcas.ac.cn

J. He
e-mail: hjm@mail.iggcas.ac.cn

Y. Yin
China Geological Survey, Beijing 100037,
People's Republic of China

H. Qian
Institute of Crustal Dynamics, China Earthquake Administration,
Beijing 100085, People's Republic of China



Fig. 1 CAS debris flow

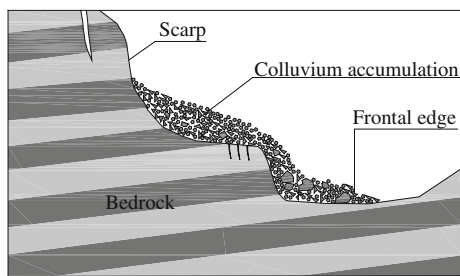


Fig. 2 Typical model of CAS

compose these accumulative formations. Discontinuity and heterogeneity are the two main characteristics of the accumulative formations because of their complex internal structure and highly non-uniform density. The macroscopic response of these kinds of accumulative formations under dynamic loading is controlled by their structure, characteristics of the grains and the disposition of contacts between them. There have been rapid advances in technology to simulate their granular behavior explicitly through DEM because of its discontinuum assumption.

2 Previous works

Recent studies in the seismic response of different types of rock or soil slopes, using different theoretical methods and models, have been carried out by several investigators. Celine Bourdeau and Hans-Balder Havenith studied seismic slope stability, 2D numerical elastic and elasto-plastic models were developed. Preliminary results suggested that the size of modeled slope failure is dependent on site effects [1]. Influence of topographical and other site specific amplification effects on the initiation of earthquake-induced slope failures were studied by Havenith et al. [2]. Nonlinear seismic response of volcanic hills using the finite element method was

studied by Sincaian and Oliveira [3], the seismic response of different parts of a hill was analyzed. 2D PFC code was used by Tang et al. [4] Hu to simulate the kinematic behavior of the Tsaoiling landslide triggered by the Chi-Chi earthquake. Athanasopoulos et al. [5] studied the effects of surface topography on seismic ground response and concluded that the characteristic surface topography played an important role in modifying the intensity of base motion in the Egion (Greece) 15 June 1995 earthquake. DEM simulations and experiments were carried out by Nishida and Tanaka to study the projectile impacting two-dimensional particle packings including dissimilar material layers. The dynamic response of a two-dimensional ordered particle packing impacted by a spherical projectile was investigated both experimentally and numerically [6]. A dynamic solution of the shear band propagation in submerged landslides was studied by Puzrin et al. Failure mechanism of submarine landslides has been investigated using the energy balance approach [7].

PFC (Particle Flow Code) developed by Itasca was employed in this paper to simulate the seismic response of accumulative formations overlying the bedrock. Particle flow models were built according to the geological investigation results carried out in quake-hit regions in Sichuan province. The horizontal component of seismic waves recorded at WoLong during the WenChuan earthquake was input into the models. The dynamic response of the different locations in the model were recorded and analyzed.

3 Numerical modeling

Numerical modeling of CAS should be based on the geological investigation carried out in the epicentral area. The formation process of these kinds of slope was summarized as following according to the results of investigations and the numerical models for the simulation were built based on the simplified results of the geometry and geology conditions on the site.

3.1 Geological framework

Colluvium accumulation is the main kind of accumulative formation in Sichuan Province and seismic shock also plays an important role during this process. The shocks not only expedite the formation process, they can also weaken the internal structure of the CAS. The historical formation process for CAS generally can be defined into 4 phases as shown in Fig. 3.

The scarp face is formed in the first phase due to the earth crust uplifting and stream erosion, interlayered rock formations outcropped along this scarp. Then the stream erosion during a relatively stationary period of earth crust movements can create valley topography in the second phase. The valley

Fig. 3 Formation process of the CAS (4 phases)

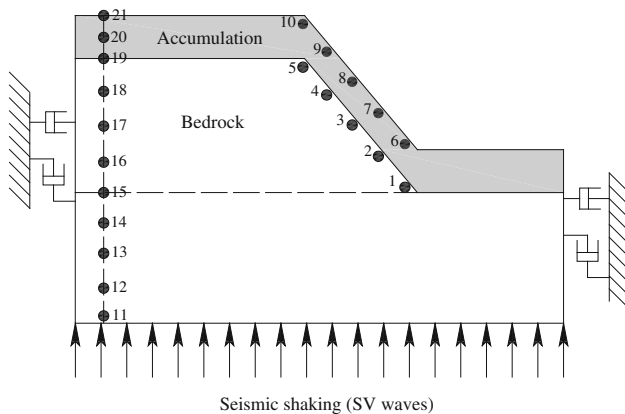
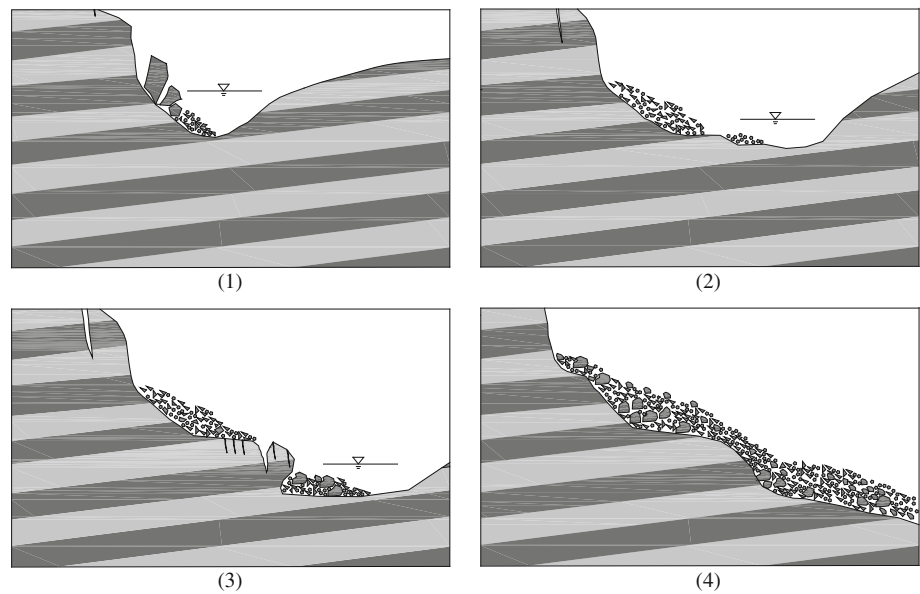


Fig. 4 Geometry and boundary conditions of the numerical model

bottom is mainly composed of weathered rock blocks. In the third phase, cavities can appear along the mudstone outcropping in the scarp face due to the debris spalling caused by differential weathering and this can lead to intermittent rock collapses. The substances produced by rock collapses are accumulated on the bedrock and exposed to the air for a long time in the last phase. Substances coating the bedrock to a certain thickness, mainly consisting of pebbles, gravel, sand and clay, are the main features of this kind of accumulation formation.

3.2 Geometry of the model

The geometry of the models is shown in Fig. 4: the surface material of colluvium accumulation with a thickness of 20 m overlying on the bedrock with a varied depth of 100 and 50 m respectively. The velocity, acceleration and displacement of the points in the model, which are marked and numbered in

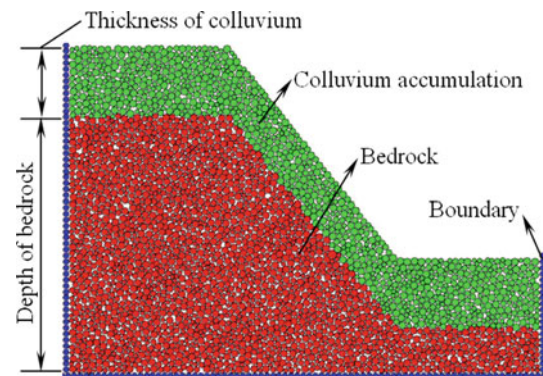


Fig. 5 A numerical model built by PFC

Fig. 4, were monitored and recorded during the whole process of simulation.

In order to analyze the seismic response of CAS, the thickness of the accumulation was kept as 20 m and the other two following parameters were varied according to the geological investigation:

- (1) The depth of the bedrock taking the values of 100 and 50 m;
- (2) The slope angle of the models taking the values of 50°, 40° and 30°.

3.3 Boundary conditions

Numerical models with varied slope angles and height were built using the PFC and one of the models is exhibited in Fig. 5. Dynamic input was applied to the base of the models by way of a velocity history. To prevent the reflection of propagating waves back into the model, larger models and a viscous boundary were used to minimize the problem. The

viscous boundary is based on the use of independent dashpots in the normal and shear directions at the lateral boundaries of the models. It is updated automatically using “while stepping” provided by FISH before the next step in the simulation process [8]. The dashpot provides viscous normal and shear tractions given by Eqs. (1) and (2):

$$f_n = -\rho C_p v_n \quad (1)$$

$$f_s = -\rho C_s v_s \quad (2)$$

where v_n and v_s are the normal and shear components of the velocity, ρ is the mass density, C_p and C_s are the P and S wave velocity. P and S wave velocity are determined through the following Eqs. (3) and (4):

$$C_p = \sqrt{\frac{E(1-\nu)}{\rho(1+\nu)(1-2\nu)}} \quad (3)$$

$$C_s = \sqrt{\frac{E}{2\rho(1+\nu)}} = \sqrt{\frac{G}{\rho}} \quad (4)$$

where E and G are the Young’s modulus and shear modulus respectively, ν is the Poisson’s ratio. In this paper we take the value of $C_p = 4500.0$ m/s and $C_s = 2800$ m/s for bedrock; $C_p = 230.0$ m/s and $C_s = 110.0$ m/s for colluvium accumulation.

3.4 Choice of parameters

PFC works at a more basic level—it synthesizes material behavior from the micro-components that make up the material [9, 10]. A contact model is used to describe the physical behavior occurring at contact. Each contact in the model consists of up to three parts: a contact-stiffness model, a slip and separation model and a bonding model [10, 11].

Parallel bonds are used to approximate the physical behavior of bedrock and overlying accumulation in the model [12, 13]. As for the parallel bond, the deformability (normal and shear stiffness) can be expressed as Eq. (3).

$$\bar{k}^n = \frac{\bar{E}_c}{L}, \quad \bar{k}^s = \frac{12I\bar{E}_c}{AL^3} \quad (5)$$

$$\bar{R} = \bar{\lambda} \min(R^{[A]}, R^{[B]}), \quad A = \pi \bar{R}^2 \quad (6)$$

where \bar{E}_c is the Young’s modulus of each parallel bond, \bar{R} is the bond radius, $\bar{\lambda}$ is the radius multiplier used to set the parallel-bond radii.

The micro material parameters of this simulation are listed in Tables 1 and 2. There are two tables of parameters for this model, Table 1 is for the bedrock and Table 2 is for the accumulation.

In PFC, the local non-viscous damping is provided and the damping force is directly added to the equations of motion as shown in Eq. (7), therefore only accelerating motion is damped and damping is frequency-independent [10]. The

Table 1 Micro parameters that define bedrock

Parameter	Description	Value
ρ	Ball density (Kg/m ³)	2,600.0
E_c	Ball-ball contact modulus (GPa)	50.0
k_n/k_s	Ball stiffness ratio	10.0
$\bar{\lambda}$	Parallel-bond radius multiplier	1.0
\bar{E}_c	Parallel-bond modulus (GPa)	50.0
\bar{k}_n/\bar{k}_s	Parallel-bond stiffness ratio	10.0
μ	Ball friction coefficient	0.5
$\bar{\sigma}_c$ (mean)	Parallel-bond normal strength, mean (MPa)	200.0
$\bar{\sigma}_c$ (SD)	Parallel-bond normal strength, SD (MPa)	50.0
$\bar{\tau}_c$ (mean)	Parallel-bond shear strength, mean (MPa)	200.0
$\bar{\tau}_c$ (SD)	Parallel-bond shear strength, SD (MPa)	50.0

Table 2 Micro parameters that define colluvium accumulation

Parameter	Description	Value
ρ	Ball density (Kg/m ³)	1,500.0
E_c	Ball-ball contact modulus (MPa)	50.0
kn/ks	Ball stiffness ratio	10.0
$\bar{\lambda}$	Parallel-bond radius multiplier	1.0
\bar{E}_c	Parallel-bond modulus (MPa)	50.0
\bar{k}_n/\bar{k}_s	Parallel-bond stiffness ratio	10.0
μ	Ball friction coefficient	0.2
$\bar{\sigma}_c$ (mean)	Parallel-bond normal strength, mean (MPa)	1.5
$\bar{\sigma}_c$ (SD)	Parallel-bond normal strength, SD (MPa)	0.15
$\bar{\tau}_c$ (mean)	Parallel-bond shear strength, mean (MPa)	1.5
$\bar{\tau}_c$ (SD)	Parallel-bond shear strength, SD (MPa)	0.15

focus of this paper is to study the seismic response instead of failure process, so relatively smaller value of 0.5 is set as the local damping coefficients in this simulation.

$$F_{(i)} + F_{(i)}^d = M_{(i)}A_{(i)} \quad (7)$$

where $F_{(i)}$, $M_{(i)}$ and $A_{(i)}$ are the generalized force, mass and acceleration components, respectively; $F_{(i)}^d$ is the damping force.

3.5 The velocity and acceleration used

WenChuan earthquake of magnitude 8.0 occurred on May 12, 2008, the East-West horizontal component of the motion, which is recorded at Wolong in the time domain of 25 s, were used in this study as the input waveform. The input seismic waves are vertically propagating SV waves applied at the bottom of the model. Therefore, the dynamic response of the CAS could be analyzed. The horizontal velocity and acceleration diagrams are shown in Figs. 6 and 7 respectively.

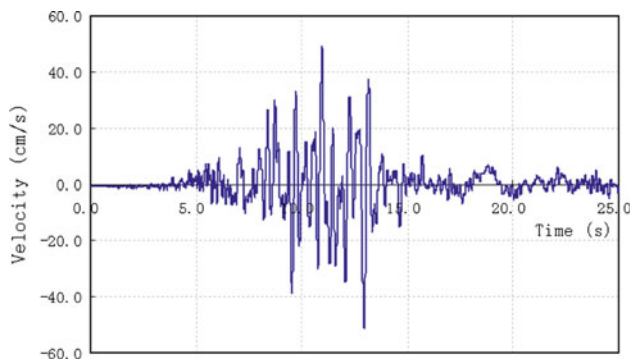


Fig. 6 The horizontal component of velocity for input (E-W)

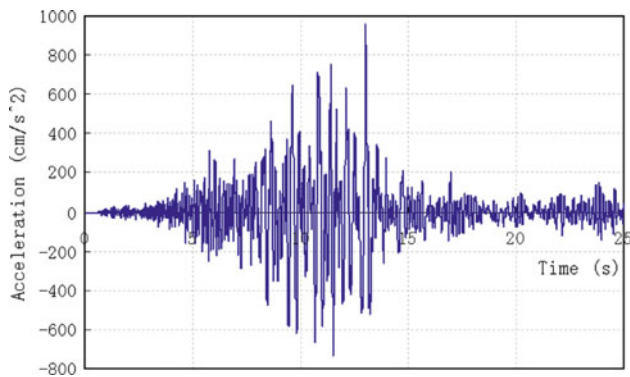


Fig. 7 The horizontal component of acceleration for input (E-W)

4 Results analysis

Six different dynamic simulations have been carried out corresponding to the possible combinations of the varied slope height and slope angle. Seismic response in terms of velocity, acceleration and displacement at the different locations in the models are presented and analyzed.

4.1 Comparison of the seismic response in colluvium and bedrock

One focus of this study is the dynamic response of the slope surface area, which is prone to sliding if the earthquake

occurs because of the existence of accumulation, so the seismic response in terms of velocity and displacement of the points 1, 3 and 5 in the accumulation and points 6, 8, 10 in the bedrock are presented in Figs. 8 to 11 respectively. Only some typical results, such as models with slope height of 120 m and slope angle of 50°, 30°, are presented here because the rest of the models show the similar seismic response.

As can be seen, there are quite different waveforms for the seismic response in terms of velocity and displacement at the points in the accumulation and bedrock. Amplification can be observed in consecutive monitored points in the models with the increase in altitude, the horizontal amplification of the displacement at the crest of the slope by reference to free-field motions is kept within 1.0–2.0 in the bedrock and it can even reach 4.0–5.0 in the accumulation. This drastic amplification effect formed in the CAS is just the reasons for so many debris flows or landslides occurred in CAS.

If the velocity waveforms are compared at points in the bedrock and accumulation, the waveforms at the different points in bedrock always keep a synchronous development. By contrast, the waveforms at the different points in accumulation show drastic change and sometimes even show a reverse development. The velocity of the points in the accumulation is much lower than the velocity of the points in the bedrock. These results revealed that the presence of surficial low-velocity colluvium accumulation is the key factor controlling ground-motions around the bedrock.

4.2 Seismic response along the vertical direction in the model

The peak velocity, acceleration and displacement at different altitudes in the model are also the concern of this study. The monitored points from 11–21 as shown in Fig. 4 were used to get the related information. The peak velocity, acceleration and displacement of the monitored points with the increase of altitude are presented in Figs. 12 and 13.

Figures 12 and 13 indicate that the peak velocity and displacement close to the interface between colluvium and

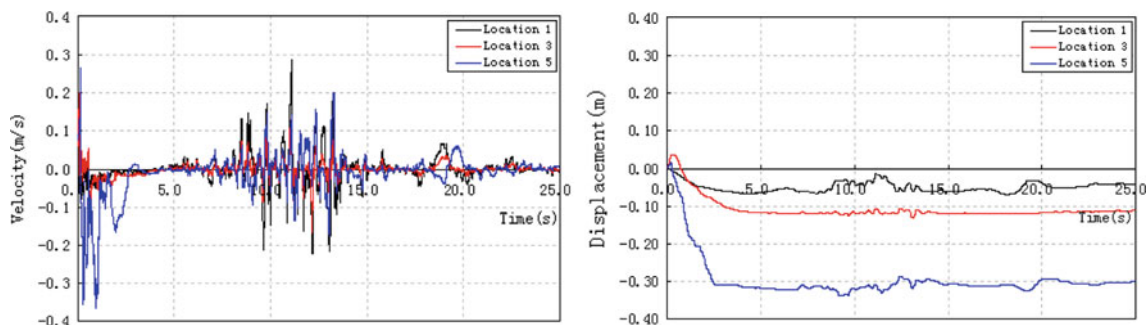


Fig. 8 Seismic response at points 1, 3 and 5 in the accumulation (slope angle: 50°)

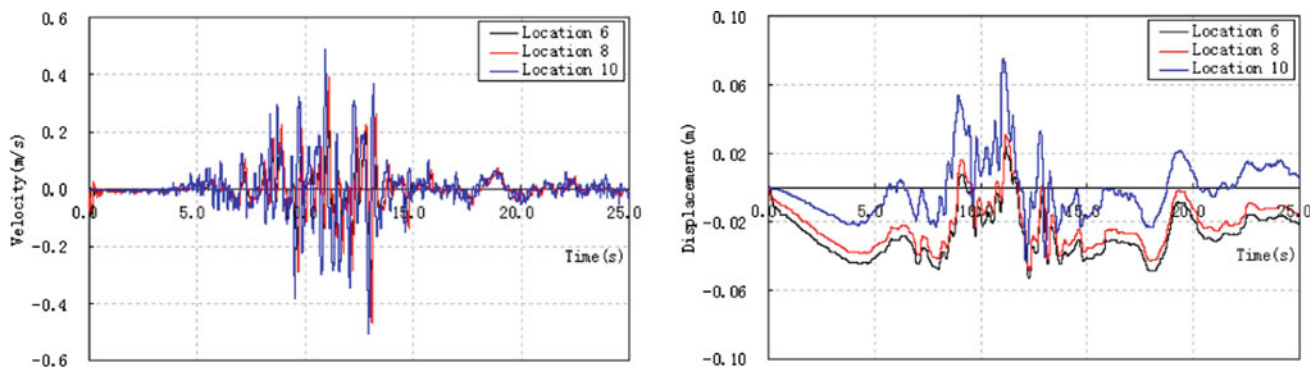


Fig. 9 Seismic response at points 6, 8 and 10 in the bedrock (slope angle: 50°)

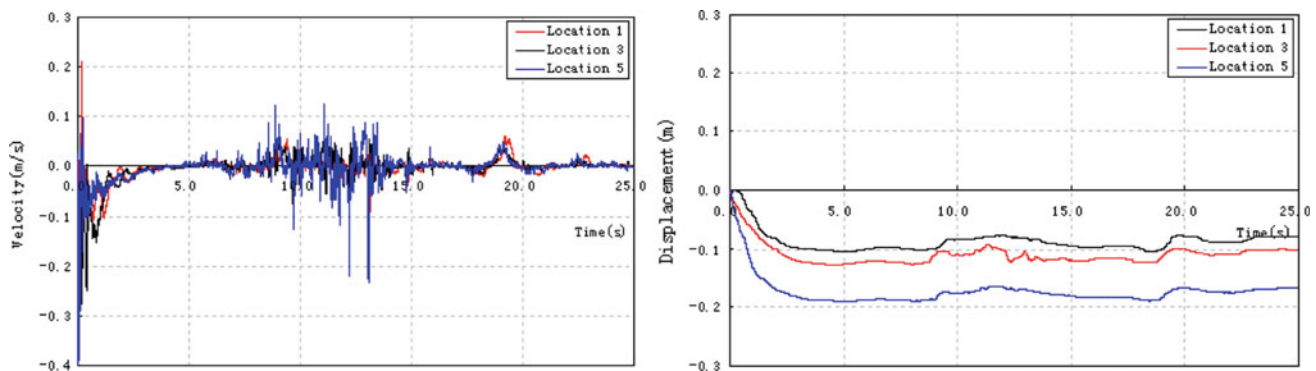


Fig. 10 Seismic response at points 1, 3 and 5 in the accumulation (slope angle: 30°)

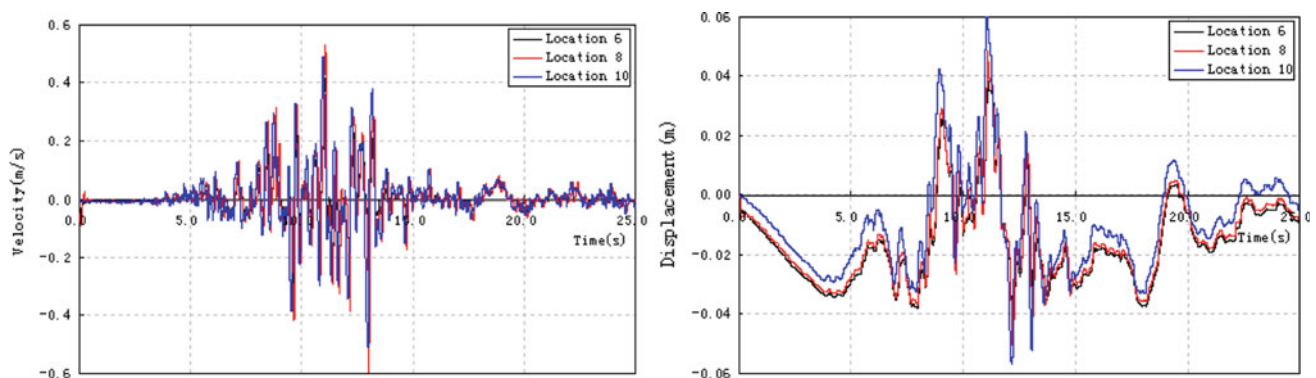


Fig. 11 Seismic response at points 6, 8 and 10 in the bedrock (slope angle: 30°)

bedrock changed drastically. Obvious amplification can be observed in bedrock and the velocity in the accumulation dropped seriously when compared with the velocity in the bedrock. It means that the surficial low-velocity colluvium accumulation is the key factor leading to the ground-motions around the bedrock. The contrasting material properties and the existence of an interface between accumulation and bedrock caused the velocity to attenuate significantly. The rapid fluctuation of the displacement in colluvium accumulation and bedrock caused by different dynamic responses can lead to the occurrence of debris flows or landslide.

5 Conclusions

Colluvium accumulation slopes (CAS) are widely distributed in the quake-hit region in Sichuan province. Earthquake induced debris flows and landslides occurring in this kind of slope represent an important risk in seismically active mountain regions, so a better understanding is necessary of the seismic response in this kin leading to such instabilities. The following conclusions can be gained through this study:

The velocity history in accumulation is much lower if compared with the bedrock. This result revealed that the

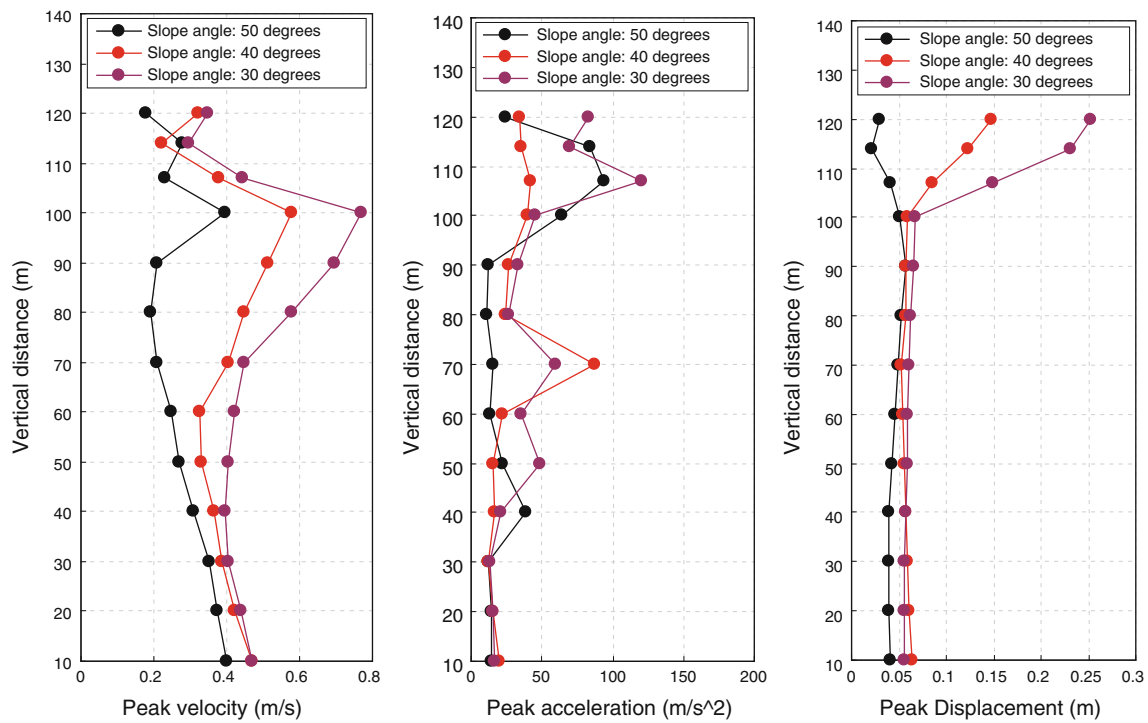


Fig. 12 Peak velocity, acceleration and displacement at different points along the vertical direction (slope height: 120m)

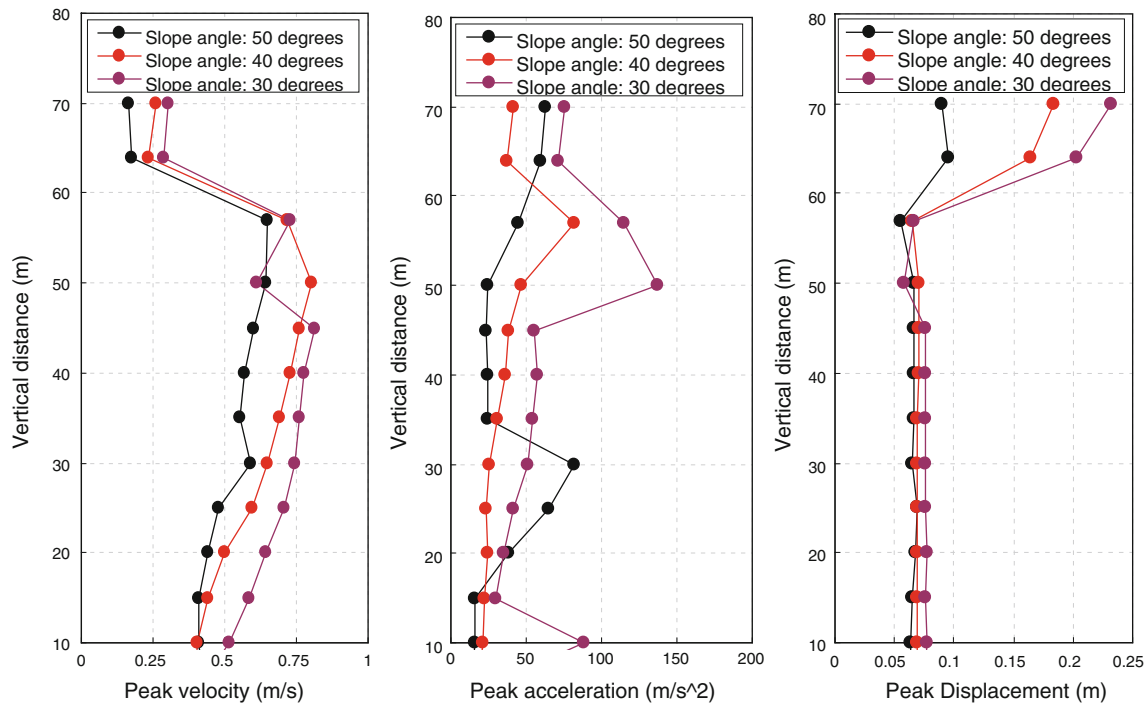


Fig. 13 Peak velocity, acceleration and displacement at different points along the vertical direction (slope height: 70m)

presence of surficial low-velocity accumulation is the key factor controlling ground-motions around the bedrock.

The contrasting material properties and the existence of the interface between accumulation and bedrock caused

the velocity to attenuate significantly. The rapid fluctuation of the displacement in colluvium accumulation and bedrock can lead to the occurrence of debris flows or landslides.

Acknowledgments The authors are grateful for financial support from the Chinese National Program of Basic Research (Project 973, No. 2009CB724605, No. 2010CB731501), China postdoctoral science foundation (20090460510), National Natural Science Foundation of China (No. 40702052), Research project of CAS (No. KZCX2-YW-JS102, KJCX3-SW-L1, YZ200912), Research project of CGS (No. 1212011014026), Principal research fund of ICDCEA (ZDJ2009-07).

References

1. Bourdeau, C., Havenith, H.-B., Fleurisson, J.-A.: Numerical modeling of seismic slope stability (2004). doi:[10.1007/b93922](https://doi.org/10.1007/b93922)
2. Havenith, H.-B., Vanini, M., Jongmans, D.: Initiation of earthquake-induced slope failures: influence of topographical and other site specific amplification effects. *J. Seismol.* **7**, 397–412 (2003)
3. Slincaian, M.V., Oliveira, C.S.: Nonlinear seismic response of a volcanic hill using the finite element method. *Soil Dyn. Earthq. Eng.* **20**, 145–154 (2000)
4. Tang, C.-L., Hu, J.-C., Lin, M.-L.: The Tsaoing landslide triggered by the Chi-Chi earthquake, Taiwan: Insights from a discrete element simulation. *Eng. Geol.* **106**, 1–19 (2009)
5. Athanopoulos, G.A., Pelekis, P.C., Leonidou, E.A.: Effects of surface topography on seismic ground response in the Egion (Greece) 15 June 1995 earthquake. *Soil Dyn. Earthq. Eng.* **18**, 135–149 (1999)
6. Nishida, M., Tanaka, Y.: DEM simulations and experiments for projectile impacting two-dimensional particle packings including dissimilar material layers. *Granular Matter* **12**(4), 357–368 (2010)
7. Puzrin, A.M., Saurer, E., Germanovich, L.N.: A dynamic solution of the shear band propagation in submerged landslides. *Granular Matter* **12**(3), 253–265 (2010)
8. Bai, X.M., Keer, L.M., Wang, Q.J.: Investigation of particle damping mechanism via particle dynamics simulations. *Granular Matter* **11**(6), 417–429 (2010)
9. Cundall, P.A., Strack, P.D.L.: A discrete numerical model for granular assemblies. *Geotechnique* **29**, 47–65 (1979)
10. Itasca Consulting Group Inc.: PFC2D Particle Flow Code. FISH in PFC. Minneapolis (2002)
11. Zhao, X.L., Evans, T.M.: Discrete simulations of laboratory loading conditions. *Int. J. Geomech.* **9**(4), 169–178 (2009)
12. Jiang, M.J., Yu, H.-S., Harris, D.: Bond rolling resistance and its effect on yielding of bonded granulates by DEM analyses. *Int. J. Numer. Anal. Methods Geomech.* **30**(7), 723–761 (2006)
13. Yasuda, N., Matsumoto, N.: Dynamic deformation characteristics of sands and rock fill materials. *Can. Geotech.* **30**, 747–757 (1993)